

# Layer intermixing in heavily carbon-doped AlGaAs/GaAs superlattices

I. Szafranek, M. Szafranek, B. T. Cunningham,<sup>a)</sup> L. J. Guido,<sup>b)</sup> N. Holonyak, Jr., and G. E. Stillman

Center for Compound Semiconductor Microelectronics, Materials Research Laboratory and Coordinated Science Laboratory, University of Illinois at Urbana-Champaign, Illinois 61801

Interdiffusion of Al and Ga in heavily C-doped  $\text{Al}_{0.3}\text{Ga}_{0.7}\text{As}/\text{GaAs}$  superlattice (SL) structures has been investigated quantitatively for a variety of ambient and surface encapsulation conditions. High-resolution photoluminescence (PL) at  $T = 1.7$  K was employed to evaluate the extent of layer intermixing after 24-h anneals at 825 °C. From the shifts to higher energies of the PL peaks due to  $n = 1$  electron-to-heavy hole transitions in the quantum wells of the annealed SLs relative to the position of this peak in the as-grown crystal, approximate Al-Ga interdiffusion coefficients ( $D_{\text{Al-Ga}}$ ) have been determined for different annealing conditions. For all encapsulants studied the interdiffusion in C-doped crystals is accelerated with increasing  $\text{As}_4$  pressure in the annealing ampoule. This result disagrees with previously observed trends for Group II-doped  $p$ -type structures, which have led to the charged point-defect model (Fermi-level effect) of Al-Ga interdiffusion. The  $\text{Si}_3\text{N}_4$  cap has provided the most effective surface sealing against ambient-stimulated layer interdiffusion, and yielded  $D_{\text{Al-Ga}} \approx 1.5 - 3.9 \times 10^{-19} \text{ cm}^2/\text{s}$ . The most extensive layer intermixing has occurred for uncapped SL annealed under As-rich ambient ( $D_{\text{Al-Ga}} \approx 3.3 \times 10^{-18} \text{ cm}^2/\text{s}$ ). These values are up to  $\sim 40$  times greater than those previously reported for nominally undoped  $\text{Al}_x\text{Ga}_{1-x}\text{As}/\text{GaAs}$  SLs, implying that the  $\text{C}_{\text{As}}$  doping slightly enhances host-atom self-diffusion on the Group III sublattice, but significantly less than predicted by the Fermi-level effect. The discrepancies between the experimental observations and the model, are discussed.

## 1. INTRODUCTION

The dependence of Al-Ga interdiffusion in quantum-well heterostructures (QWHs) on anneal ambient and surface encapsulation conditions has been extensively investigated under both intrinsic and impurity-induced regimes for  $\text{Al}_x\text{Ga}_{1-x}\text{As}/\text{GaAs}$  and related III/V material systems (for a recent review, see Ref. 1). Based on results of that work a consistent picture has evolved, whereby the self-diffusion of Group III host atoms, which causes the layer intermixing, is presumably mediated by the Group III vacancy ( $V_{\text{III}}$ ) and interstitial ( $I_{\text{III}}$ ) charged native point defects.<sup>1-5</sup> The concentrations of these defects depend on the Fermi-level position and crystal stoichiometry, and can be experimentally controlled by doping and/or the anneal ambient atmosphere.<sup>1-5</sup> Specifically, Al-Ga interdiffusion has been found to increase in  $n$ -type superlattice (SL) crystals with heavy doping of either Group IV (e.g., Si)<sup>4</sup> or Group VI (e.g., Se)<sup>6</sup> substitutional donors during anneals under As-rich ambient, both conditions enhancing solubility of the negatively charged  $V_{\text{III}}$ . On the other hand, when a SL is  $p$ -type with a heavy doping of Group II on Ga sublattice elements (e.g., Mg),<sup>4</sup> increased interface smearing has been observed after Ga-rich anneals, supposedly because of an excess concentration of positively charged  $I_{\text{III}}$  defects.<sup>1-5</sup>

Recent advances in heavy carbon doping of GaAs and  $\text{Al}_x\text{Ga}_{1-x}\text{As}$  grown by metalorganic chemical vapor deposition (MOCVD)<sup>7,8</sup> have allowed, for the first time, tests of

the trends outlined above also for this Group IV on As sublattice acceptor species.<sup>9</sup> In that work<sup>9</sup> the extent of Al-Ga interdiffusion was found to be extremely small compared to other  $p$ -type dopants, and could not be detected with conventional microanalytical techniques such as cross-sectional two-beam transmission electron microscopy (TEM) or secondary-ion mass spectrometry (SIMS). This led to the conclusion that heavy  $\text{C}_{\text{As}}$  doping suppresses layer disordering in  $\text{Al}_x\text{Ga}_{1-x}\text{As}/\text{GaAs}$  SLs relative to an undoped crystal. Also, using low-resolution photoluminescence (PL) at  $T = 77$  K, lack of interdiffusion enhancement under Ga rich compared to As-rich annealing conditions was observed.<sup>9</sup> These recent results obviously disagree with previous data on impurity-induced layer disordering (ILD) in general, and the Fermi-level (or charged point-defect) interdiffusion model,<sup>2-5</sup> in particular.

Because of the central importance of the data on ILD in heavily C-doped SL crystals to the understanding of the Group III self-diffusion, we have performed a more complete, quantitative study of anneal ambient and surface encapsulation effects on this process. In this work low-temperature, weak-excitation PL has been employed for improved spectral resolution. The layer disordering-induced shifts to higher energies ( $\Delta E$ ) of the  $n = 1$  electron-to-heavy hole ( $e \rightarrow hh$ ) confined-particle transitions were analyzed to yield Al-Ga interdiffusion coefficients ( $D_{\text{Al-Ga}}$ ) for different annealing conditions at  $T = 825$  °C. This work confirms one of the major conclusions of the earlier study.<sup>9</sup> We have observed clear trends of enhanced interface smearing in SLs annealed under As rich relative to As-deficient ambients for all cases of crystal surface sealing. However, the calculated values of  $D_{\text{Al-Ga}}$  (825 °C) fall in the range of

<sup>a)</sup> Now at Sandia National Laboratories, Division 1141, Albuquerque, NM 87185.

<sup>b)</sup> Now at Yale University, Department of Electrical Engineering, Center for Microelectronic Materials and Structures, Box 2157 Yale Station, New Haven, CT 06520.

$\sim 1.5 \times 10^{-19} - 3.3 \times 10^{-18} \text{ cm}^2/\text{s}$ , which is higher than the previously reported  $D_{\text{Al-Ga}} \approx 8 - 10 \times 10^{-20} \text{ cm}^2/\text{s}$  for undoped SLs.<sup>3</sup> This indicates a slight enhancement of the interdiffusion process in the C-doped crystals relative to intrinsic conditions (for a compilation of the latter data see Ref. 3). Thus, although a weak IILD effect is operative in heavily C-doped  $p$ -type  $\text{Al}_{0.3}\text{Ga}_{0.7}\text{As}/\text{GaAs}$  SLs in agreement (at least qualitative) with the Fermi-level model,<sup>2-5</sup> a revision is required with regard to the identity of the native defects that may be responsible for the Group III self-diffusion in the presence of large concentrations of substitutional acceptor impurities on the As sublattice.

## II. EXPERIMENTAL PROCEDURE

The SL crystal investigated here was grown by low-pressure MOCVD in an EMCORE GS3100 reactor on a  $2^\circ$  off (100) oriented liquid-encapsulated Czochralski GaAs substrate. Trimethylgallium, trimethylaluminum, and 100% arsine were the growth precursors, and the carbon doping source was a 500-ppm mixture of  $\text{CCl}_4$  (Matheson) in high-purity  $\text{H}_2$ .<sup>7</sup> The flow rates of  $\text{CCl}_4 \approx 100 \text{ sccm}$  and  $\text{H}_2 \approx 9 \text{ slm}$  resulted in an approximately uniform carbon doping level of  $[\text{C}] \approx 8 \times 10^{18} \text{ cm}^{-3}$  throughout the whole epitaxial multilayer stack of GaAs and  $\text{Al}_x\text{Ga}_{1-x}\text{As}$ , as confirmed by SIMS concentration depth profiles. The growth was carried out at  $T \approx 620^\circ\text{C}$ , pressure  $p \approx 100 \text{ Torr}$ , growth rate  $\approx 500 \text{ \AA}/\text{min}$ , V/III ratio  $\approx 160$ , and substrate rotation rate  $\approx 1500 \text{ rpm}$ . The SL crystal consists of a  $\sim 700\text{-\AA}$ -thick GaAs buffered layer, followed by 40  $\text{Al}_{0.3}\text{Ga}_{0.7}\text{As}/\text{GaAs}$  periods of equal barrier and well thicknesses  $L_B \approx L_Z \approx 200 \text{ \AA}$ . The SL is confined with a  $\sim 200\text{-\AA}$   $\text{Al}_{0.8}\text{Ga}_{0.2}\text{As}$  layer and further capped with a  $\sim 200\text{-\AA}$  GaAs layer.

The anneals were performed in evacuated quartz ampoules (volume  $\approx 3 \text{ cm}^3$ ,  $p \approx 10^{-6} \text{ Torr}$ ) at  $T = 825^\circ\text{C}$  for 24 h. Three sets of samples were annealed in separate ampoules under different conditions of the crystal surface stoichiometry: (i) As-rich ambient (+ As), achieved by adding 25 mg of elemental As resulting in an  $\text{As}_4$  overpressure of about 2.5 atm in the sealed ampoule at  $825^\circ\text{C}$ ; (ii) Ga-rich conditions (+ Ga), maintained by placing an elemental Ga in the ampoule to create a very As-deficient ambient corresponding to the equilibrium between the  $\text{As}_4$  vapor from the SL crystal and the excess Ga at  $T = 825^\circ\text{C}$ ; and (iii) equilibrium GaAs conditions (+ 0), existing when neither As nor Ga is added to the ampoule, so that the more volatile As atoms evaporate from the crystals until equilibrium is reached between the vapor and the Ga-rich epitaxial crystal surface. A set of three samples was loaded into each ampoule. Two SL crystals were encapsulated with an  $\sim 1000\text{-\AA}$ -thick layer of either  $\text{SiO}_2$  or  $\text{Si}_3\text{N}_4$  deposited by CVD at  $\sim 400$  and  $\sim 700^\circ\text{C}$ , respectively, and the third sample had an uncapped surface.

The carrier concentration depth profile in the as-grown SL was measured with Polaron PN4200 capacitance-voltage electrochemical profiler. The as grown and some annealed samples were analyzed also with TEM and SIMS. As asserted earlier, these techniques did not provide much useful information concerning the layer intermixing process. The

TEM data confirmed the precalibrated thicknesses  $L_B \approx L_Z \approx 200 \text{ \AA}$  in the as-grown SL crystal.

The optical properties of all the samples were assessed with low-temperature PL. The samples were mounted strain free in superfluid  $^4\text{He}$  at  $T \approx 1.7 \text{ K}$ . Low-level excitation ( $\sim 36 \text{ mW}/\text{cm}^2$ ) using the  $5145\text{-\AA}$  line from an  $\text{Ar}^+$  laser, was employed. An unfocused beam of about 3 mm in diameter was used to probe almost the entire area of the samples, thus averaging over possible lateral inhomogeneities of the crystals. The emitted radiation was dispersed by an Instruments SA 1-m double spectrometer and detected by a thermoelectrically cooled GaAs photomultiplier tube, using the photon counting technique.

## III. DATA ANALYSIS

The dominant feature in the low-temperature PL spectrum of the as-grown SL crystal shown in Fig. 1 (dashed curve) is a single, broad peak (full width at half maximum FWHM  $\approx 17.6 \text{ meV}$ ) at  $\sim 1.5316 \text{ eV}$ . This peak is attributed to  $n = 1$  electron-to-heavy hole ( $e \rightarrow hh$ ) confined-particle recombination in GaAs quantum wells. The observed emission energy matches within 0.1 meV the value for a square-wave potential in a multiple QWH, calculated using the algorithm of Kolbas and Holonyak<sup>10</sup> with boundary conditions modified to satisfy continuity of  $(1/m^*)d\Psi/dz$ , in order to account for different effective masses across the well/barrier heterointerfaces.<sup>11,12</sup> The parameters used in the calculations are:  $L_B = L_Z = 200 \text{ \AA}$ ,  $x_Z(\text{Al}) = 0$ ,  $x_B(\text{Al}) = 0.3$ ,  $m_e^* = 0.0665 + 0.0835x$ ,<sup>13,14</sup>  $m_{hh}^* = 0.34$

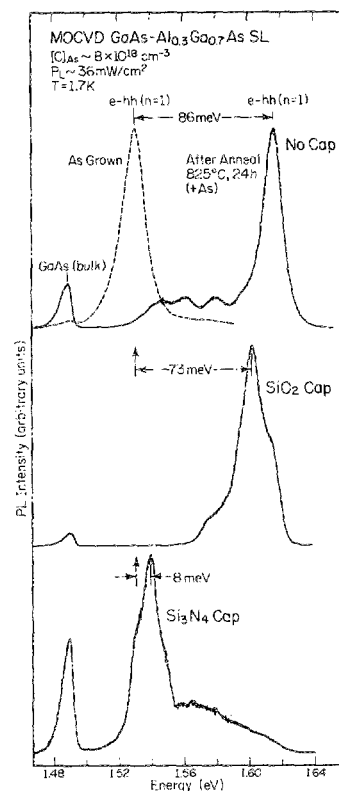


FIG. 1. Photoluminescence spectra of the as-grown (dashed line) and annealed heavily C-doped  $\text{Al}_{0.3}\text{Ga}_{0.7}\text{As}/\text{GaAs}$  superlattice crystals. The effect of surface encapsulation on Al-Ga interdiffusion efficiency under As-rich annealing ambient is demonstrated by variations in the energy shift of the  $(e \rightarrow hh)_{n=1}$  emission relative to the as-grown sample. A stable low-energy peak at  $\sim 1.49 \text{ eV}$  due to bulk GaAs is also shown.

+ 0.42x,<sup>13,14</sup>  $E_g(x) = E_g(\text{GaAs}) + 1.247x$ ,<sup>15</sup>  $E_g(\text{GaAs}) = 1.5192 \text{ eV}$  at  $T = 1.7 \text{ K}$ ,<sup>16</sup> and the conduction band-edge discontinuity  $\Delta E_c = 0.6\Delta E_g$ .<sup>13,17</sup> The deviation of  $\sim 0.1 \text{ meV}$  in the calculated transition energy corresponds roughly to a 1% error in  $m^*$  or to a fraction of a monolayer ( $< 2 \text{ \AA}$ ) uncertainty in  $L_z$ . Since the actual uncertainties in values of all the parameters are much greater than that (e.g., at least  $\pm 10 \text{ \AA}$  for  $L_z$  and  $L_B$ ), the fit accuracy of  $\sim 1 \text{ meV}$  is sufficient for our purposes.

For  $L_z = 200 \text{ \AA}$ , the binding energies of both free and neutral acceptor-bound heavy-hole excitons are  $\sim 7 \text{ meV}$ .<sup>18</sup> If the main SL peak observed experimentally (Fig. 1) were due to annihilation of these excitons, this would imply an  $(e \rightarrow hh)_{n=1}$  energy between  $\sim 7$  to  $\sim 14 \text{ meV}$  higher than the calculated value. However, it should be pointed out that the specified barrier and well dimensions are the lower limits of these quantities, as determined from growth calibration, TEM and SIMS. Furthermore, the TEM image of the as-grown SL shows abrupt interfaces. Finally, computer simulations indicate that correction to the calculated  $(e \rightarrow hh)_{n=1}$  photon energy due to inaccuracy in  $x_B$  (or  $\Delta E_g$ ) should be at most of the order of  $\sim 1 \text{ meV}$ . It is, therefore, impossible to account for an underestimate as large as  $\sim 7\text{--}14 \text{ meV}$ , and we conclude that despite the low temperature of  $1.7 \text{ K}$ , formation of free excitons and their subsequent capture at C acceptors are suppressed in these SL crystals, presumably due to delocalization effects caused by the high doping level.<sup>19</sup> It follows, that the SL-related transition observable in PL spectrum of the as-grown sample originates most probably in the  $(e \rightarrow hh)_{n=1}$  recombination process, as asserted at the beginning of this section.

The PL spectra of the annealed SLs also exhibit a single prominent transition at  $h\nu > E_g(\text{GaAs})$ , accompanied by usually weak shoulders and secondary peaks on both high- and low-energy sides (Fig. 1). The important assumption underlying our analysis is that the dominant SL peaks in the PL spectra of the as grown and annealed crystals are of the same origin. With this assumption, we can deduce the Al-Ga interdiffusion coefficients from the measured shifts to higher energies  $\Delta E$  of the emission lines in the annealed SLs relative to the as-grown one, as discussed later. The additional, weaker spectral features seen in Fig. 1 may result from depth-dependent extent of layer intermixing,<sup>20</sup> giving rise to a wide range of confined-particle bound states detected with PL.

The large depth penetration of the PL probe is manifested directly by the presence of a broadband at  $\sim 1.49 \text{ eV}$ , also shown in Fig. 1. This transition comes from unresolved conduction band-to-acceptor ( $e-A^0$ ) and donor-to-acceptor ( $D^0-A^0$ ) recombination processes due to C acceptors in the bulk GaAs, namely the cap and buffer layers, as well as the substrate. The latter assignment has been supported by the PL spectra measured from the back surface of the substrate. The observation of occasionally very intense GaAs luminescence through the  $\sim 1\text{-}\mu\text{m}$ -thick SL stack indicates a large ambipolar diffusion length of the photogenerated carriers and/or a photon recycling effect.<sup>21</sup> The peak position of this transition is invariant with annealing conditions, thus confirming that it is not related to the SL structure, and provid-

ing an intrinsic calibration of the extent of Al-Ga interdiffusion in each case of annealing conditions. Moreover, changes in the relative intensity of this peak may serve as a sensitive monitor of varying transport properties of the annealed SL crystals.

The energy shift  $\Delta E$  due to layer disordering-induced modification of the SL composition profile after annealing under given conditions allows an approximate determination of the corresponding Al-Ga interdiffusion coefficient,  $D_{\text{Al-Ga}}$ .<sup>22-24</sup> We have employed the general solutions of Fick's equation with constant  $D_{\text{Al-Ga}}$  using Fourier series expansion<sup>25</sup> to satisfy the initial conditions of the periodic square-well potential profile, and the boundary condition;

$$x(z, t \rightarrow \infty) = (L_B x_B + L_z x_z) / (L_z + L_B).$$

The Schrödinger equation, with the modified kinetic energy operator  $\{ - (\hbar^2/2) (\partial/\partial z) [1/m^*(z)] (\partial/\partial z) \}$  used to account for spatially varying effective masses,<sup>11,12</sup> was solved for the lowest eigenvalues in the smoothed periodic conduction and heavy-hole valence bands, assuming a symmetric envelope wave function as described by Lee, Schlesinger, and Kuech.<sup>24</sup> The number of Fourier components included in the characteristic matrix of the eigenvalue problem was increased until the convergence criterion of the relative change of  $< 0.1\%$  in energy of the lowest bound state was met. For each measured value  $\Delta E$  a conjugate gradient iterative procedure was applied to find  $D_{\text{Al-Ga}}$  such that  $|\Delta E_{\text{exp}} - \Delta E_{\text{calc}}| < 0.1 \text{ meV}$ . An example of the potential profiles for the as grown and two annealed SL structures shown in Fig. 1, as well as the corresponding  $n = 1$  confined-particle bound states and  $(e \rightarrow hh)_{n=1}$  transitions are presented schematically in Fig. 2.

This method is very sensitive to the SL structural parameters. For example, an uncertainty of about one monolayer in  $L_z \approx 200 \text{ \AA}$  causes up to 10% change in  $D_{\text{Al-Ga}}$  in the low-diffusivity regime of  $\sim 10^{-19} \text{ cm}^2/\text{s}$ . However, the high accuracy ( $\sim 0.2 \text{ meV}$ ) in the PL data is sufficient to draw unambiguous conclusions with regard to the influence of the surface encapsulation and annealing ambient on the extent of AlGaAs/GaAs heterointerface disordering.

## IV. EXPERIMENTAL RESULTS

### A. Surface encapsulation effects

Photoluminescence measurements examining the effects of encapsulation on the extent of interface smearing in the SLs capped with  $1000\text{-}\text{\AA}$ -thick  $\text{SiO}_2$  and  $\text{Si}_3\text{N}_4$  films relative to the unprotected sample are shown in Fig. 1 for the (+ As) anneal ambient. As discussed in the following section, the As-rich atmosphere significantly enhances the interdiffusion in the C-doped crystals, and hence it offers the most sensitive conditions for evaluation of the influence of the encapsulation on retarding the SL disordering. Equivalent trends were observed also for the other two annealing ambients studied, however.

The most extensive SL composition profile grading leading to the greatest PL energy shift observed in this work,  $\Delta E \approx 86 \text{ meV}$ , occurred for the capless sample, as shown in the top spectrum of Fig. 1. The  $\text{SiO}_2$  cap is permeable to Ga

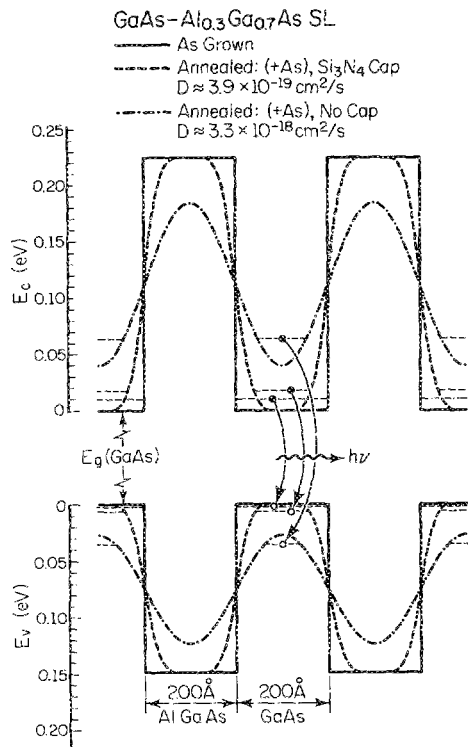


FIG. 2. Potential energy profiles of  $\text{Al}_{0.3}\text{Ga}_{0.7}\text{As}/\text{GaAs}$  SL before (square wave, solid line) and after 24-h-long anneal under (+ As) ambient with  $\text{Si}_3\text{N}_4$  cap (dashed curve) and with no cap (chained line), based on the data presented in Fig. 1 and Table I. The horizontal dashed lines show the confined-particle bound states calculated for each potential profile. Also indicated are the  $(e \rightarrow hh)_{n=1}$  transitions corresponding to the measured photoluminescence.

and, thus, provides a very ineffective surface encapsulation relative to the uncapped crystal.<sup>26-28</sup> This effect of Ga out-diffusion induced-layer intermixing can be seen in Fig. 1, where  $\Delta E \approx 73$  meV for  $\text{SiO}_2$  cap is the second largest SL peak energy shift measured in our study.

As expected, the most efficient encapsulation against Al-Ga interdiffusion stimulated by crystal interaction with the ambient atmosphere was provided by the  $\text{Si}_3\text{N}_4$  cap.<sup>26,28</sup> The most extensive interface grading after 24-h anneal with this encapsulant was observed again for the (+ As) ambient, but it resulted in a PL energy shift only of  $\sim 8$  meV, as shown in the bottom spectrum of Fig. 1. Our data indicate that the  $\text{Si}_3\text{N}_4$  layer, although relatively nonporous, does not entirely block in- and out-diffusion of Al, Ga, and As, since a clear dependence of  $\Delta E$  on the annealing ambient has been observed for the  $\text{Si}_3\text{N}_4$  cap as well, as summarized in Table I.

## B. Anneal ambient effects

Regardless of crystal encapsulation, an obvious monotonic trend of decreasing extent of layer intermixing on transition from As-rich to As-deficient (or Ga-rich) annealing conditions is evident in our data. This is demonstrated in Fig. 3 for  $\text{SiO}_2$ , capped, and in Fig. 4 for capless SL crystals. In both cases significant variations in the PL energy shifts relative to the as-grown sample can be noticed as a function

TABLE I. Peak energy up-shifts of the  $(e \rightarrow hh)_{n=1}$  transitions in annealed C-doped  $\text{Al}_{0.3}\text{Ga}_{0.7}\text{As}/\text{GaAs}$  SL crystals relative to the as-grown sample, and the corresponding Al-Ga interdiffusion coefficients at  $T = 825^\circ\text{C}$ , for different encapsulation and ambient conditions.

Cap	Annealing ambient		
	(+ Ga)	(+ 0)	(+ As)
None	$\Delta E$ (meV)	27–38	N/A
	$D$ ( $\text{cm}^2/\text{s}$ )	$1.1\text{--}1.5 \times 10^{-18}$	$3.3 \times 10^{-18}$
$\text{SiO}_2$	$\Delta E$ (meV)	31	59
	$D$ ( $\text{cm}^2/\text{s}$ )	$1.3 \times 10^{-18}$	$2.2 \times 10^{-18}$
$\text{Si}_3\text{N}_4$	$\Delta E$ (meV)	3.1	6.7
	$D$ ( $\text{cm}^2/\text{s}$ )	$1.5 \times 10^{-19}$	$3.3 \times 10^{-19}$

of the anneal ambient. As mentioned above, a similar behavior has been observed also for the  $\text{Si}_3\text{N}_4$ -capped samples, but in this case over a much narrower spectral range of  $\sim 3 \leq \Delta E \leq 8$  meV. The spectroscopic data and the corresponding calculated values of  $D_{\text{Al-Ga}}$  are summarized in Table I.

## V. DISCUSSION

The PL data and the corresponding Al-Ga interdiffusion coefficients for the whole matrix of the C-doped SL crystals annealed under different ambient conditions with various surface encapsulants, are summarized in Table I. Using a similar approach, Schlesinger and Kuech<sup>23</sup> and Lee

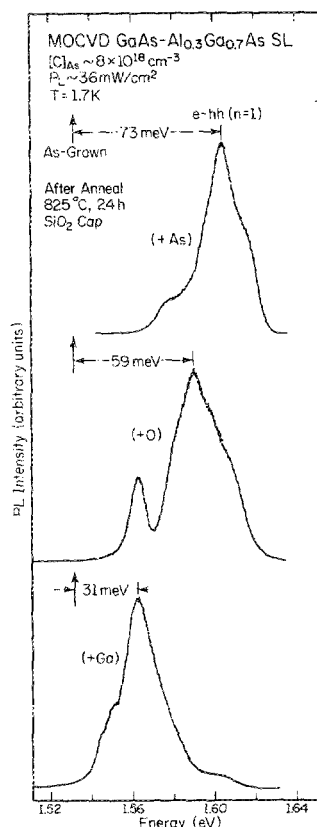


FIG. 3. Photoluminescence spectra of heavily C-doped  $\text{Al}_{0.3}\text{Ga}_{0.7}\text{As}/\text{GaAs}$  superlattice crystals annealed with  $\text{SiO}_2$  cap under (+ As), (+ 0), and (+ Ga) ambients. A monotonic trend of enhanced layer disordering with increasing  $\text{As}_4$  pressure in the ampoule is evident by comparing the energy shifts of the dominant SL luminescence from each annealed sample relative to that of the as-grown sample.

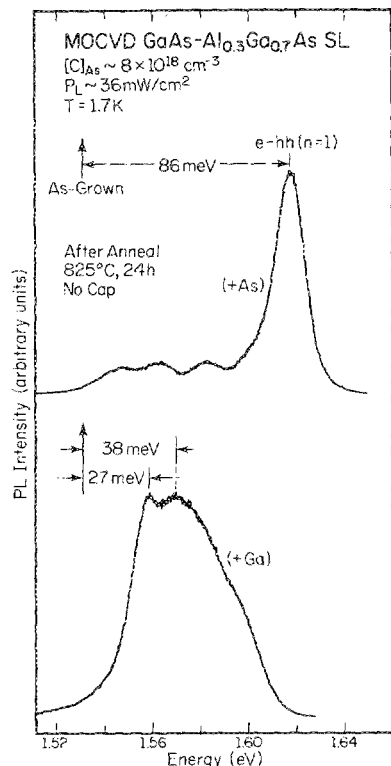


FIG. 4. Photoluminescence spectra of heavily C-doped  $\text{Al}_{0.3}\text{Ga}_{0.7}\text{As}/\text{GaAs}$  superlattice crystals annealed with uncapped surface under (+ As) and (+ Ga) ambients. A clear trend of enhanced layer disordering with increasing  $\text{As}_4$  pressure in the ampoule is evident by comparing the energy shifts of the dominant SL luminescence from each annealed sample relative to that of the as-grown sample.

and co-workers,<sup>24</sup> determined  $D_{\text{Al-Ga}} \approx 9.7 \times 10^{-20} \text{ cm}^2/\text{s}$  for a nominally undoped  $\text{Al}_{0.3}\text{Ga}_{0.7}\text{As}/\text{GaAs}$  quantum-well system annealed with  $\text{Si}_3\text{N}_4$  cap at  $825^\circ\text{C}$ . Tan and Gösele<sup>3</sup> compiled the available data on Ga self-diffusion and Al-Ga interdiffusion under intrinsic conditions and obtained  $D_{\text{Al-Ga}}(825^\circ\text{C}) \approx 8.4 \times 10^{-20} \text{ cm}^2/\text{s}$ . Our results range from  $D_{\text{Al-Ga}} = 1.5\text{--}3.9 \times 10^{-19} \text{ cm}^2/\text{s}$  for  $\text{Si}_3\text{N}_4$  caps to  $D_{\text{Al-Ga}} = 1.1\text{--}3.3 \times 10^{-18} \text{ cm}^2/\text{s}$  for the samples with uncapped surfaces, over the whole investigated range of  $\text{As}_4$  pressure in the ampoules. These diffusivity values are higher than those for undoped crystals, indicating an effect of slight impurity-induced layer disordering enhancement in C-doped  $p$ -type  $\text{AlGaAs}/\text{GaAs}$  SLs. We believe that the present quantitative conclusion is more reliable than that recently published,<sup>9</sup> which was based on a qualitative evaluation of TEM images. From simulations of a SL composition profile as a function of Al-Ga interdiffusion we have noticed that for typical SL structures used in our IILD studies (e.g., Refs. 4, 9, and this work), the transition from a high TEM alloy contrast to a practically irresolvable image may take place over a less than one order of magnitude range of  $D_{\text{Al-Ga}}$ .

The relatively weak interdiffusion enhancement measured in our work is quantitatively consistent with earlier results for Be-doped and implanted SLs,<sup>29-31</sup> as discussed by Tan and Gösele,<sup>2,3</sup> as well as with our estimate of the lower bound of  $D_{\text{Al-Ga}} \approx 5 \times 10^{-17} \text{ cm}^2/\text{s}$  in Mg-doped crystal reported by Deppe *et al.*<sup>4</sup> In all these cases the observed IILD effect is significantly less extensive than the  $D_{\text{Al-Ga}} \propto (p/n_i)^\alpha$  dependence predicted by the Fermi-level model,<sup>2,3,5</sup> where  $\alpha = +2$  is the charge state of the Group III interstitials.<sup>32</sup> The measured values of  $D_{\text{Al-Ga}}$  set an upper limit of  $\alpha = 1$ ,

thus clearly disagreeing with the charged point-defect model.<sup>2-5</sup>

Furthermore, Ralston *et al.*<sup>31</sup> reported a significant difference between the effect of implanted Be vs Mg on layer intermixing. Similarly, Deppe *et al.*<sup>4</sup> demonstrated a complete destruction of a Mg-doped SL structure after a 10-h anneal at  $815^\circ\text{C}$  under (+ 0) ambient which, as mentioned above, corresponds to a lower bound of  $D_{\text{Al-Ga}} \approx 5 \times 10^{-17} \text{ cm}^2/\text{s}$ . This value is more than one order of magnitude greater than the highest  $D_{\text{Al-Ga}}$  value determined in this work for the C-doped crystals (Table I). These discrepancies indicate dopant species dependence of IILD in  $p$ -type SLs. In particular, they suggest that a negligible enhancement of Al-Ga interdiffusion in C and some Be-doped  $p$ -type crystals with grown-in (as opposed to diffused-in) dopants is probably not a general effect, and as such it lacks a proper explanation by the Fermi-level model.

The dependence of the interdiffusion efficiency on annealing ambient in heavily C-doped SLs reported in this paper raises additional questions with regard to the charged-defect model in its present form.<sup>1-5</sup> The model implies that the doping level and type, by determining the Fermi-level position,<sup>2,3</sup> and the annealing atmosphere, by affecting the crystal stoichiometry,<sup>1,4,5</sup> are the dominant factors controlling the concentration of the charged defects which are believed to assist in Group III self-diffusion, namely Group III vacancies ( $V_{\text{III}}$ ) and interstitials ( $I_{\text{III}}$ ). The model predicts that because of the electronic energy contribution to the total free energy of a semiconductor, the layer disordering in  $p$ -type materials proceeds via the interstitialcy mechanism involving positively charged, donorlike  $I_{\text{III}}$ . A strong enhancement of the interdiffusion in Mg-doped SLs annealed under Ga rich relative to As-rich surface conditions,<sup>4</sup> has seemed to directly support such a notion. However, the unambiguous trend of increasing layer intermixing with increasing  $\text{As}_4$  pressure [ $p(\text{As}_4)$ ] in the annealing ambient, that we have observed for heavily C-doped  $p$ -type SLs with all analyzed forms of surface encapsulation, obviously contradicts the  $D_{\text{Al-Ga}} \propto [1/p(\text{As}_4)]^{1/4}$  dependence predicted by the Fermi-level model.<sup>5</sup>

A plausible explanation for the observed IILD enhancement under As-rich conditions is that other point defects, and in particular As interstitial  $I_{\text{As}}$  and As antisite defect  $\text{As}_{\text{III}}$  become active in Al-Ga interdiffusion mechanism in the presence of Group IV majority substitutional impurities on the As sublattice. For example, annihilation of  $I_{\text{As}}$  on a Group III sublattice can generate  $I_{\text{III}}$  and  $\text{As}_{\text{III}}$  via the kick-out process,



thus bringing about an excess nonequilibrium concentration of  $I_{\text{III}}$  defects even under (+ As) anneal ambient. Since all the point defects in Eq. (1) are donorlike,<sup>32</sup> their solubility is expected to be relatively high in  $p$ -type crystals. Moreover, Coulomb interaction between the positively charged  $\text{As}_{\text{III}}$  and  $I_{\text{III}}$ , as well as a Group III concentration gradient due to the very As-rich surface which acts as a  $I_{\text{III}}$  sink boundary, would then enhance  $I_{\text{III}}$  out-diffusion and, consequently,

layer disordering. Naturally, because of very low absolute concentrations of the defects in Eq. (1), this process is not expected to be as effective as may be the case for a highly soluble and diffusive Group II impurity such as Zn. The latter species, which can be present in relatively large concentrations in crystal while occupying both substitutional and interstitial sites, participate directly in diffusion of Group III sublattice host and dopant atoms through the interstitialcy mechanism.<sup>2,3,5</sup>

## VI. CONCLUSIONS

The first quantitative data on impurity-induced layer intermixing of AlGaAs/GaAs SLs in heavily C-doped crystals have been reported for different surface encapsulation and annealing ambient conditions. As expected, the Si<sub>3</sub>N<sub>4</sub> cap provided the best surface encapsulation and reduced the extent of IILD by about one order of magnitude compared to both uncapped and SiO<sub>2</sub>-capped crystals. A slight enhancement of  $D_{\text{Al-Ga}}$  for  $[C] \approx 8 \times 10^{18} \text{ cm}^{-3}$  has been observed relative to previously published results for nominally undoped SL structures.<sup>3</sup> However, the extent of layer intermixing is quantitatively inconsistent with the Fermi-level model,<sup>2-5</sup> which significantly overestimates the  $D_{\text{Al-Ga}}$  values.

For all surface encapsulation conditions studied, a monotonic trend of increasing  $D_{\text{Al-Ga}}$  with increasing  $p(\text{As}_4)$  in an ampoule has been observed. This behavior is opposite to that predicted by the charged point-defect model<sup>2-5</sup> and, therefore, it suggests that the model in its present form, where the Al-Ga interdiffusion in  $p$ -type crystals is assumed to be mediated mainly by Group III interstitials, lacks general validity.

Finally, a twofold species dependence of IILD has been discussed: (i) a significant difference in the absolute magnitude of  $D_{\text{Al-Ga}}$  in Mg vs C-doped SLs for nominally the same concentrations of these two acceptor impurities; and (ii) an opposite dependence of layer intermixing on the annealing ambient in these two cases. The species dependence is not accounted for at all by the Fermi-level effect model<sup>2-5</sup> in its present form.

## ACKNOWLEDGMENTS

Helpful discussions with J. S. Major, Jr., as well as the technical assistance of M. K. Suits, R. MacFarlane, and R. T. Gladin in preparation of this manuscript are appreciated. This work was supported by the Joint Services Electronics Program, under Contract No. N00015-84-C-0149, by the National Science Foundation, under Grant Nos. DMR 86-

12860 and CDR 85-22666 and by SDIO/IST under Contract No. DAAL 03-89-K-0080 administered by the Army Research Office.

- <sup>1</sup> D. G. Deppe and N. Holonyak, Jr., J. Appl. Phys. **64**, R93 (1988).
- <sup>2</sup> T. Y. Tan and U. Gösele, J. Appl. Phys. **61**, 1841 (1987).
- <sup>3</sup> T. Y. Tan and U. Gösele, Appl. Phys. Lett. **52**, 1240 (1988).
- <sup>4</sup> D. G. Deppe, N. Holonyak, Jr., W. E. Plano, V. M. Robbins, J. M. Dallsasse, K. C. Hsieh, and J. E. Baker, J. Appl. Phys. **64**, 1838 (1988).
- <sup>5</sup> R. M. Cohen, J. Appl. Phys. **67**, 7268 (1990).
- <sup>6</sup> D. G. Deppe, N. Holonyak, Jr., K. C. Hsieh, P. Gavrilovic, W. Stutius, and J. Williams, Appl. Phys. Lett. **51**, 581 (1987).
- <sup>7</sup> B. T. Cunningham, M. A. Haase, M. J. McCollum, and G. E. Stillman, Appl. Phys. Lett. **54**, 1905 (1989).
- <sup>8</sup> B. T. Cunningham, J. E. Baker, and G. E. Stillman, Appl. Phys. Lett. **56**, 836 (1990).
- <sup>9</sup> L. J. Guido, B. T. Cunningham, D. W. Nam, K. C. Hsieh, W. E. Plano, J. S. Major, Jr., E. J. Vesely, A. R. Sugg, N. Holonyak, Jr., and G. E. Stillman, J. Appl. Phys. **67**, 2179 (1990).
- <sup>10</sup> R. M. Kolbas and N. Holonyak, Jr., Am. J. Phys. **52**, 431 (1984).
- <sup>11</sup> W. A. Harrison, Phys. Rev. **123**, 85 (1961).
- <sup>12</sup> D. J. BenDaniel and C. B. Duke, Phys. Rev. **152**, 683 (1966).
- <sup>13</sup> R. C. Miller, D. A. Kleinman, and A. C. Gossard, Phys. Rev. B **29**, 7085 (1984).
- <sup>14</sup> P. Lavaetz, Phys. Rev. B **4**, 3460 (1971).
- <sup>15</sup> H. C. Casey, Jr. and M. B. Panish, *Heterostructure Lasers: Part A; Fundamental Principles* (Academic, Orlando, 1978), p. 192.
- <sup>16</sup> D. D. Sell, Phys. Rev. B **6**, 3750 (1972).
- <sup>17</sup> M. A. Haase, M. A. Emanuel, S. C. Smith, J. J. Coleman, and G. E. Stillman, Appl. Phys. Lett. **50**, 404 (1987).
- <sup>18</sup> D. C. Reynolds, K. K. Bajaj, C. W. Litton, P. W. Yu, W. T. Masselink, R. Fischer, and H. Morkoc, Phys. Rev. B **29**, 7038 (1984).
- <sup>19</sup> P. J. Dean and D. C. Herbert, in *Excitons*, edited by K. Cho (Springer, Berlin, 1979), p. 131.
- <sup>20</sup> L. J. Guido, N. Holonyak, Jr., K. C. Hsieh, and J. E. Baker, Appl. Phys. Lett. **54**, 262 (1989).
- <sup>21</sup> J. L. Bradshaw, W. J. Choyke, R. P. Devaty, and R. L. Messham, J. Appl. Phys. **67**, 1483 (1990).
- <sup>22</sup> M. D. Camras, N. Holonyak, Jr., R. D. Burnham, W. Streifer, D. R. Scifres, T. L. Pauli, and C. Lindström, J. Appl. Phys. **54**, 5637 (1983).
- <sup>23</sup> T. E. Schlesinger and T. Kuech, Appl. Phys. Lett. **49**, 519 (1986).
- <sup>24</sup> J.-C. Lee, T. E. Schlesinger, and T. F. Kuech, J. Vac. Sci. Technol. B **5**, 1187 (1987).
- <sup>25</sup> J. Crank, *The Mathematics of Diffusion*, 2nd ed. (Clarendon/Oxford University, London, 1975), p. 17.
- <sup>26</sup> K. V. Vaidyanathan, M. J. Helix, D. J. Wolford, B. G. Streetman, R. J. Blattnier, and C. A. Evans, Jr., J. Electrochem. Soc. **124**, 1781 (1977).
- <sup>27</sup> D. G. Deppe, L. J. Guido, N. Holonyak, Jr., K. C. Hsieh, R. D. Burnham, R. L. Thornton, and T. L. Paoli, Appl. Phys. Lett. **49**, 510 (1986).
- <sup>28</sup> L. J. Guido, J. S. Major, Jr., J. E. Baker, W. E. Plano, N. Holonyak, Jr., and K. C. Hsieh, J. Appl. Phys. **67**, 6813 (1990).
- <sup>29</sup> M. Kawabe, N. Shimizu, F. Hasegawa, and Y. Nannichi, Appl. Phys. Lett. **46**, 849 (1985).
- <sup>30</sup> Y. Hirayama, Y. Suzuki, and H. Okamoto, Jpn. J. Appl. Phys. **24**, 1498 (1985).
- <sup>31</sup> J. Ralston, G. W. Wicks, L. F. Eastman, B. C. De Cooman, and C. B. Carter, J. Appl. Phys. **59**, 120 (1986).
- <sup>32</sup> G. A. Baraff and M. Schlüter, Phys. Rev. Lett. **55**, 1327 (1985).